

Effect of pH and Ionic Exchange on the Reactivity of Bioglass/Chitosan Composites Used as a Bone Graft Substitute

Samira Jebahi, Hassane Oudadesse, Eric Wers, Jiheun Elleuch, Hafedh Elfekih, Hassib Keskes, Xuan Vuong Bui, Abdelfatteh Elfeki

Abstract—Chitosan (CH) material reinforced by bioactive glass (46S6) was fabricated. 46S6 containing 17% wt% CH was studied *in vitro* and *in vivo*. Physicochemical techniques, such as Fourier transform infrared spectroscopy (FT-IR), coupled plasma optical emission spectrometry (ICP-OES) analysis were used. The behavior of 46S6CH17 was studied by measuring the *in situ* pH in a SBF solution. The 46S6CH17 was implanted in the rat femoral condyl. *In vitro* 46S6CH17 gave an FTIR - spectrum in which three absorption bands with the maxima at 565, 603 and 1039cm⁻¹ after 3 days of soaking in physiological solution. They are assigned to stretching vibrations of PO₄³⁻ group in phosphate crystalline. Moreover, the pH measurement was decreased in the SBF solution. The stability of the calcium phosphate precipitation depended on the pH value. *In vivo*, a rise in the Ca and phosphate P ions concentrations in the implanted microenvironment was determined.

Keywords—Bioglass, Chitosan, pH measurement, Hydroxyapatite Carbonated Layer.

I. INTRODUCTION

IN recent years, functional biomaterial research has been directed towards the development of improved biomaterials and new drug delivery systems. In this regard, considerable attention has been given to chitosan (CH)- based materials [1], [2]. Chitosan is a natural polymer which can be obtained by the partial deacetylation of chitin [3]. One of the properties of CH is that it can be molded in various forms [4]. CH possesses an excellent ability to form porous structures. Porous biomaterials are generated by freezing and lyophilizing CH solutions [5]-[7]. The use of chitosan for tissue engineering as a scaffolding material has also been reported [8]. However, chitosan is mechanically weak and

lacks bioactivity, which severely limits its biomedical applications. Bioactive glasses are an excellent candidate materials for bone repair and regeneration because when immersed in a physiological solution [9], [10], these bioactive materials can form an amorphous calcium phosphate layer and then crystallize to hydroxyl carbonate apatite (HCA) which has a similar chemical composition and structure to the mineral phase of human bone [11], [12]. This phenomenon is also observed during *in vivo* experiments [13]. The formation of apatite layer allows a chemical bonding between implant biomaterials and bone tissues. For this reason, it is desirable to develop a composite material with bioglass matrices associated with chitosan. In this study, the bioglass materials were used as powder fillers to reinforce the chitosan biomaterial. The studying of the pH changes in the solution helped in the explanation of the general mechanism of the bioactive process involving Bioglass. One study reported that the solubility of hydroxyapatite depended on temperature, the concentrations of calcium and phosphate and pH [14]. According to them, the silica gel was not stable when the pH increased to above 9.5. However, the stability of the calcium phosphate precipitation increased with pH [15]. A high pH environment was favorable for hydroxyapatite nucleation rate approached to that of octacalcium phosphate at pH 10 [16]. In the present study, we wanted to analyze the dissolution and reprecipitation processes of 46S6CH17. The determination of their *in vitro* behavior was studied by measuring the *in situ* pH inside the particle beds in simulated body fluid (SBF). The *in vivo* analyses were performed to determine whether the materials was tolerant in the *Wistar* rat model and whether an apatite layer was formed on the composite surfaces after implantation.

TABLE I
CONCENTRATION OF SBF SOLUTION

Ion	Na ⁺	K ⁺	Ca ²⁺	Mg ²⁺	Cl ⁻	HCO ₃ ³⁻	HPO ₄ ²⁻
SBF	142.0	5.0	2.5	1.5	148.8	4.2	1.0
Plasma	142.0	5.0	2.5	1.5	103.0	27.2	1.0

II. MATERIALS AND METHODS

A. Biomaterials Synthesis

First, the bioactive glass particle was synthesized via the melting method [17]. To synthesize 46S6CH17 biocomposite,

Jebahi Samira is with the University of Rennes 1, UMR CNRS 6226, 263 Avenue du General Leclerc, 35042 Rennes Cedex, France (phone: 0021653762227; fax: 0021674 274 437; e-mail: jbahisamira@yahoo.fr).

Hassane Oudadesse, Xuan Vuong Bui, and Eric Wers are with the University of Rennes 1, UMR CNRS 6226, 263 Avenue du General Leclerc, 35042 Rennes Cedex, France.

Jiheun Elleuch and Slim Tounsi are with the Laboratory of Human Molecular Genetics, Faculty of Medicine, University of Sfax, Sfax, Tunisia.

Hafedh Elfekih is with the Science Materials and Environment laboratory, Sfax Faculty of Science, Sfax, Tunisia.

Hassib Keskes is with the Orthopaedic and Traumatology laboratory Sfax Faculty of Medicine Sfax, Tunisia.

Abdelfatteh Elfeki is with the Animal Ecophysiology Laboratory, Sfax Faculty of Science, Department of Life Sciences, Sfax, Tunisia.

the chitosan polymer with a medium molecular weight was dissolved in 1% acetic acid aqueous solution (Sigma, France) during 2 hours at room temperature. Mixture of bioactive glass particles and chitosan polymer was stirred during 2 hours at room temperature using magnetic stirring at 1,200rpm (round per minute). After eliminating surplus solution, the mixture was frozen by liquid azotes and placed into a freeze drying during 24 hours to totally exclude solvent. The obtained composite was immersed in 10% NaOH solution for two hours and washed several times with deionized water in order to neutralize the residues of acetic acid. Finally, the composite was frozen by liquid azotes and freeze-dried again for 24 hours to completely remove water.

B. Physicochemical Analyses

1. *In vitro* Assays in Simulated Body Fluid (SBF)

The *in vitro* bioactivity of the 46S6 glass and of the 46S6CH17 was verified by the method previously described for bioactive glasses [18]. *In vitro* experiments were realized by soaking 250mg of powder in 50mL of simulated body fluid (SBF) as shown in Table I with ionic concentrations and pH nearly equal to those of human plasma at the same temperature (37°C). The samples were taken out the fluid; after short time periods (4, 8 hours) and after long ones (1, 2, 5, 15 and 30 days) of soaking. The chemical compositions of the solutions, in which the glass samples were analyzed using inductively coupled plasma optical emission spectrometry (ICP-OES) (Ciros; Spectro Analytical Instrument, Germany) to evaluate the calcium and phosphorous ions exchange between the samples and the solutions.

C. Animals and Experimental Design

Female Wistar rats (16–19 weeks of age), were used in this study. The rats were fed on a pellet diet (Sicco, Sfax, Tunisia) and water *ad libitum*. All the animals were kept under climate-controlled conditions (25°C; 55% humidity; 12h of light alternating with 12h of darkness). All rats were randomly divided into 3 groups, the first group (I) used as control (T). Groups II, III were implanted respectively with 46S6 and 46S6CH17 implant. Anesthesia was induced with xylazine (7 to 10mg/kg (i.p) ROMPUN® 2%) and ketamine (70 to 100mg/kg (i.m) imalgene®) depending on the body weight. A drilled hole, 3mm diameter and 4mm deep, was created on the lateral aspect of the femoral condyle using a refrigerated drill to avoid necrosis. Both 46S6 and 46S6CH17 were sterilized by γ irradiation from a ^{60}Co Source gamma irradiation at a dose of 25 Gy (Theratron external beam teletherapy, Equinox, Ottawa, ON, Canada) implant. The drill-hole was filled with 10mg of biomaterials. The filling was done carefully in a retrograde fashion to ensure both minimal inclusion of air bubbles and direct implant – bone contact. The rats were obtained from the central pharmacy, Tunisia, and bred in the central animal house. The handling of the animals was approved by the Tunisian ethical committee for the care and use of laboratory animals.

D. Analysis Methods

several physicochemical methods such as Fourier transform infrared spectroscopy FTIR (Bruker Equinox 55), Scanning Electron Microscopy SEM (Jeol JSM 6301F) and inductively coupled plasma optical emission spectrometry ICP-OES (Ciros; Spectro Analytical Instrument, Germany) were employed for the analysis of the 46S6 and 46S6CH17 glasses after soaking in synthetic physiological liquid (SBF) and after *in vivo* implantation at different time intervals.

III. RESULTS AND DISCUSSIONS

A. ICP-OES Results

Figs. 1 and 2 show the variations of Ca, and P concentrations, measured by ICP-OES method, in SBF versus the soaking time after contact with 46S6CH17 samples. In fact, for 46S6, calcium ion concentration increases very strongly from 100ppm to 153ppm during the first day of immersion. This increase is coherent with the release of available calcium content from bioactive glass in the desalkalization process. The calcium ion concentration increases gently till the second day, and then it decreases very strongly till the last day of immersion (30 days).

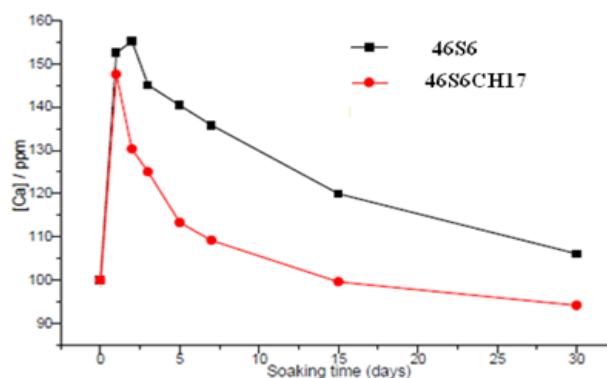


Fig. 1 Evolution of elemental concentrations of Ca in SBF solution measured by ICP-OES, versus soaking times

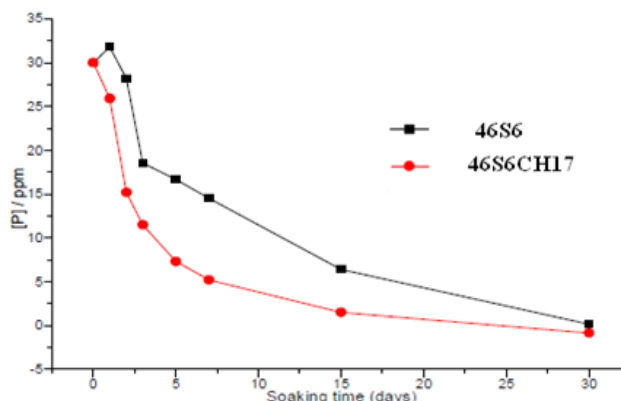


Fig. 2 Evolution of elemental concentrations of P in SBF solution measured by ICP-OES, versus soaking times

For 46S6CH17 biocomposite, calcium ion concentration increases strongly during the first day of immersion from 100ppm to 148ppm. The increase is lower than that of 46S6. This could be attributed to the presence of chitosan polymer that prevents the calcium ion dissolution. Regarding the phosphorus concentration, a maximum is reached after 8h of immersion in the case of 46S6. The phosphorus ion concentration augments with a small quantity after the first day of immersion. It corresponds to dissolution of a small quantity of phosphorus from the matrix of bioactive glass. Furthermore, the phosphorus ion concentration decreases very fast till the last day of immersion because the phosphorus is used to form the layer of calcium phosphate on the surface of pure bioactive glass. On the other hand, 46S6CH17 biocomposite does not present an increase of the phosphorus ion concentration after the first day of immersion. It is probably due to the presence of chitosan that retards the dissolution of bioglass from the matrix. After 30 days of immersion, the phosphorus ion concentration is decreases until the zero value in SBF solution. The *in vivo* characterization of newly -formed bone demonstrated that in the 46S6CH17 implanted group, Ca concentration was increased from 262 to 245mg/g (Fig. 3).

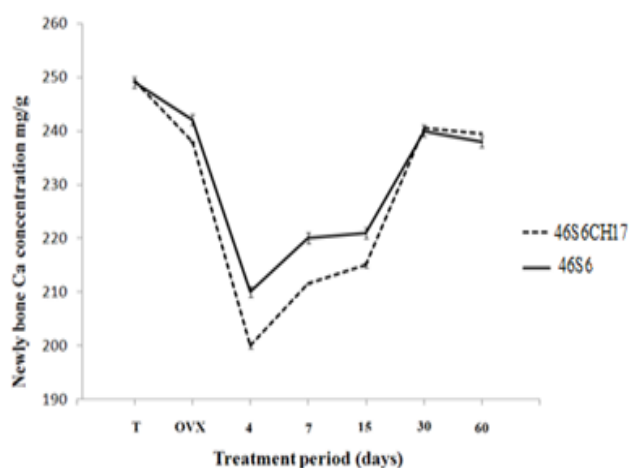


Fig. 3 Evolution of Ca concentrations in newly-formed *Wistar* rats bone implanted with bioglass (46S6) and bioglass associated with chitosan (46S6CH17) for 4, 7, 15, 30 and 60 day

These results corroborated the P content measurements whose investigation showed at about 139 and 145mg/g after 15 and 30 days, respectively (Fig. 4).

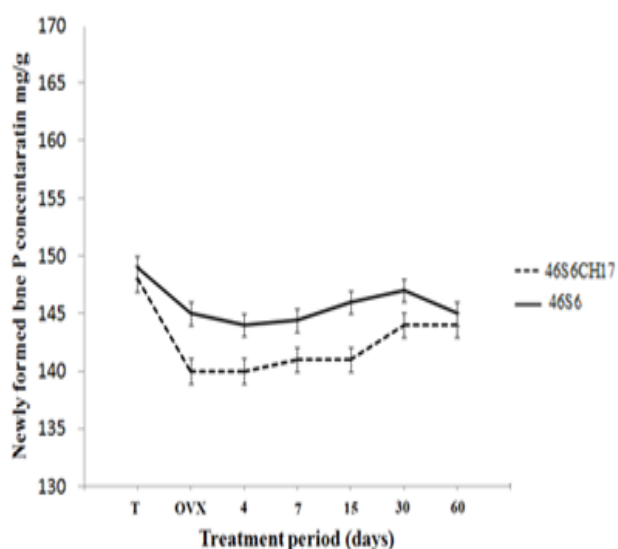


Fig. 4 Evolution of P concentrations in newly formed *Wistar* rats bone implanted with bioglass (46S6) and bioglass associated with chitosan (46S6CH17) for 4, 7, 15, 30 and 60 days

This layer indicated the 46S6CH17 bioactivity. This composite formed a chemical bond with the bone tissue resulting in a very strong bone/ 46S6CH17 interface. In fact, under scanning electron microscopy, Fig. 8 allows to visualize the pore network. It was observed that 46S6CH17 had average pore sizes of approximately 10 μ m in diameter. Pores could be expected to afford space for bone in growth.

B. Transmission-FTIR Results and pH Measurement

A peak at 800cm⁻¹ is clearly visible; this is related to the formation of silica-like structure (SiOSi). After 3 days, the shoulder at 600cm⁻¹ seems to become more pronounced, indicating that a more complete amorphous calcium phosphate layer is beginning to form (Fig. 5).

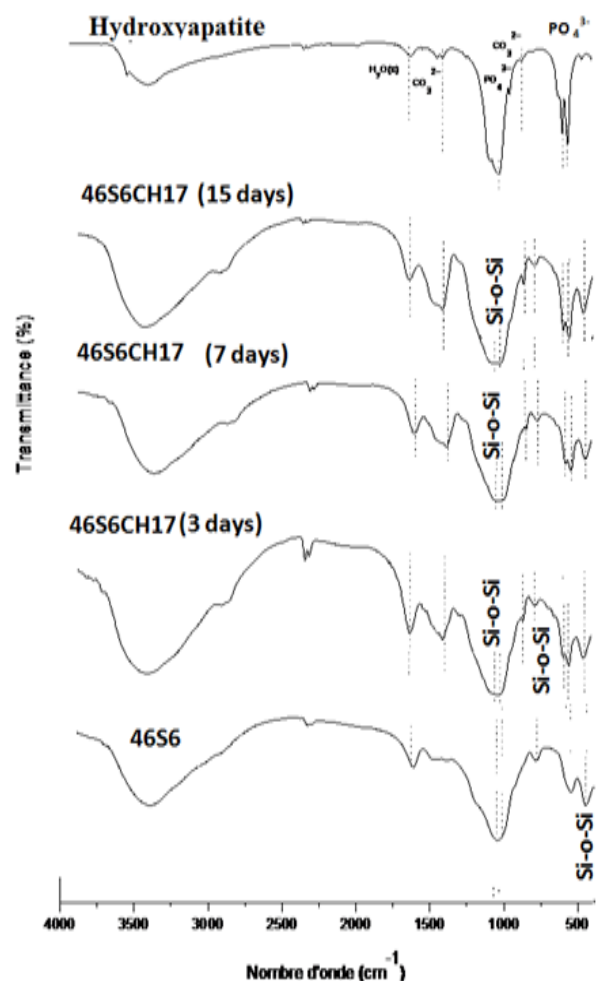


Fig. 5 FTIR spectra of 46S6CH17 after 3, 7 and 15 days after SBF immerse

The phosphate precipitation occurs more on the sample reacted at alkaline pH [19]. The higher pH is, the higher the carbonation is, as can be seen by peaks at 1500 and 872cm^{-1} . In fact, the latter is observed only on samples reacted at pH 9, and is assigned to the ν_2 vibration of CO bond [20]. The larger formation of CaCO_3 at pH 9 is consistent with the explanation previously suggested for the decrease in pH observed in these solutions. These authors observed a similar trend of reactivity by changing the powder/solution volume ratio in SBF solution [21]. As they reported, a higher concentration of the material in solution caused a greater increase in pH, and this implied that calcium carbonate formed at the expense of CHA. In Fig. 6, an increase in pH occurring in the earliest period of the dissolution was seen. ICP data confirm that the exchange of Na^+/H^+ ions is responsible for the increase in pH. In fact, the pH immediately increases nearly another pH unit in the following 4h. In the previous literature, a decrease in pH of bioglass dissolution was observed after the first 6h of reaction [22].

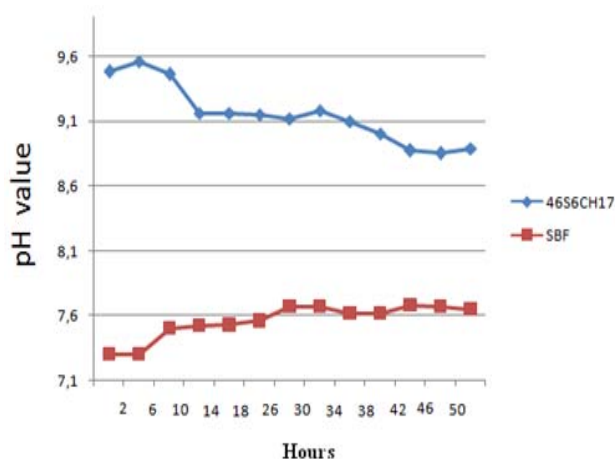
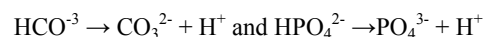


Fig. 6 The pH of the SBF solution, the 46S6CH17 after SBF immersion solution as a function of the time

The reason for this decrease can be explained by considering the precipitation of calcium phosphates and carbonates: the uptake of carbonate and phosphate ions shifts the equilibrium



towards the products side, thus causing a decrease in the pH. The formation of this peak is related to the calcium phosphate precipitation [23] and is in good agreement with the decrease in P observed with ICP-OES after a similar time. In the literature, the rate of pH increase inside the particle beds depended on the particle size and the immersion progression. In one study [24] the pH in the samples with the finest particle size ($<45\mu\text{m}$) was much higher than the values for the coarser particle fractions. Regarding the largest size fraction ($800\text{--}1000\mu\text{m}$), the pH measurement showed a much lower value. The difference in the layer formation was assumed to depend on the ion concentration of the SBF to which the particles had been exposed. In the present study, the powder particles, sized between $40\text{--}63\mu\text{m}$ verify the pH value. Similar results based on Fourier transform infrared spectra of the reaction layers on bioactive glass particles have been reported by [25]. In general, the reactions of the glass particles followed the steps proposed by Hench et al. [26]. The particles started to leach and dissolve immediately when in contact with SBF. The rapid release of alkali ions was assumed to cause the similarly rapid increase in pH inside the solution. With prolonged immersion, the rapid increase in the interfacial pH was slowed down by the reaction layers that developed on the glass surfaces, as suggested by the SEM observations. The pH changes measured in this study were in well agreement with observations of immersion of glass 45S5 particles [27] in which a rapid increase in pH took place in the solution during the first 2–6h, after which the pH either gradually increased or slightly decreased. In one study, [28] assumed that the poor layer formation on the smaller particles was due to the rapid increase in pH, which altered the solubilization and

subsequent repolymerization of the Si-rich layer, which is necessary to form the calcium phosphate layer.

C. MEB Morphology Results

Fig. 7 presents SEM micrographs of 46S6 and 46S6CH17 surfaces. The morphology of the surface layer is quite similar for both compositions, presenting particles packed in spherical aggregates. However, for the same soaking time, the observed cracks on 46S6CH17 surface are broader and more regular than on 46S6 ones. This observation is in relation with an increase of the silica gel layer thickness. The surfaces of the investigated samples are almost completely covered by the apatite crystals, especially on the surface of the 46S6CH17 biocomposite where thick layer of apatite is being observed. It is recognized that the hydroxyapatite layers formed on the surfaces of 46S6CH17 biocomposite is more dense and visible than the one over the 46S6 material. This confirms the well crystallization of apatite layer on the surface of 46S6CH17 biocomposite.

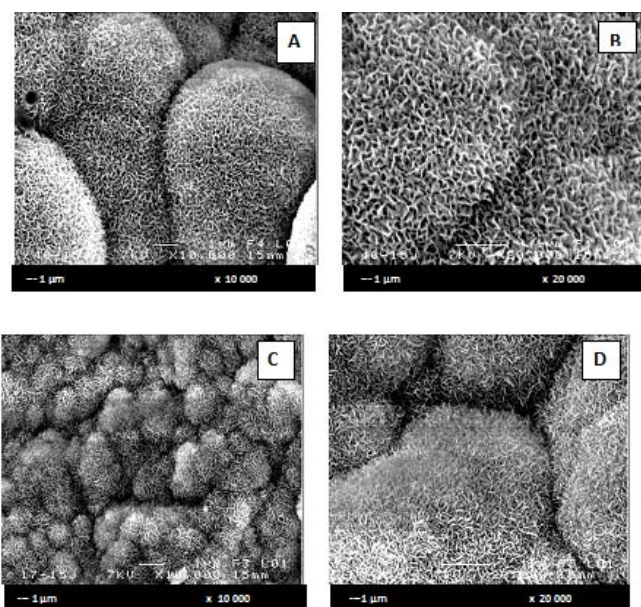


Fig. 7 SEM images of bioactive glass (BG) (a), (b) and BG/CH biocomposite (c), (d) after 15 days of soaking in SBF solution (X 10000 and 20000)

The association of chitosan with bioactive glass creates the positive effects to improve the formation and the crystallization of hydroxyapatite layer. The *in vivo* investigation with SEM showed the deposition of significant amounts of mineralized matrix, with a significant increase of Ca-P. The 46S6CH17 was replaced by creeping substitution and a mature newly generated bone appeared at the defect site.

In the newly formed bone biological HAP was deposited in an orderly way on a collagenous matrix as we noted the biodegradation of interconnection with neighboring cells (Fig. 8).

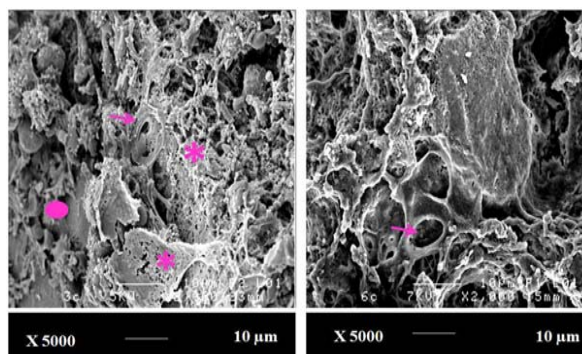


Fig. 8 SEM image of bone-implant in female Wistar rat 7 days post surgery. * Indicates BG-CH osseointegration. Arrows point indicates BG-CH pore. Circle indicates bone

IV. CONCLUSION

The greatest increase in pH was observed during the first 4 h of immersion. With prolonged immersion, the pH inside the particle beds decreased slightly. The *in vitro* assays demonstrated the bioactivity of the composite material, with the formation of a CHA layer. The *in vivo* study demonstrated that 46S6CH17 is safe and well tolerated by the host. New bone progressively forms on the implants surface and incorporates into the host bone showing that 46S6CH17 has excellent biocompatibility and has proven an effective osseointegration.

REFERENCES

- [1] R.A. Muzzarelli, F. Tanfani, M. Emanuelli, D. P. Pace, E. Chiumzzi, "Sulfated n-(carboxymethyl) chitosans: novel blood anticoagulants," *Carbohydr Res.*, Vol.126, NO.2, pp.225-31, Mar. 1984.
- [2] X.D. Liua, S. Tokurab, N. Nishia, N. Sakairi, "A novel method for immobilization of chitosan onto nonporous glass beads through a 1,3-thiazolidine linker", *J Polymer.*, Vol. 44, NO.4, pp. 1021-1026. Feb. 2003.
- [3] M. Guiping, DongzhY. i, Kennedy J. F., Jun N., "Synthesize and characterization of organic-soluble acylated chitosan", *Carbohydr Polym.*, VOL. 75, NO.3. PP. 390-394, Feb. 2009.
- [4] N. Annabi, J. W. Nichol, Zhong X , C. Ji, S. Koshy, A. Khademhosseini, F. Dehghani, "Controlling the Porosity and Microarchitecture of Hydrogels for Tissue Engineering", *Eng Part B Rev.*, VOL. 16, NO.4. PP. 371-383, Aug. 2010.
- [5] G. Chen, T. Ushida, T. Tateishi., "Development of biodegradable porous scaffolds for tissue engineering". *J. Mater Sci Eng C.*, Vol. 5, NO.2. pp.77-83, Jun. 2002.
- [6] D. Eberli, F. L. Freitas, A. Atala, J. J. Yoo., "Composite scaffolds for the engineering of hollow organs and tissues". *Methods*, VOL. 47, NO.2.PP. 109-15, Feb. 2009.
- [7] A. Bahetia, L. Kumarb, A.K.Bansal., J "Excipients used in lyophilization of small molecules". *Excipients and Food Chem.*, VOL. 1, NO.1.PP. 41, Jun. 2010.
- [8] WW. Thein-Han, J. Saikhun, C Pholpramoo, R. D. Misra, Y. Kitiyanant, "chitosan-gelatin scaffolds for tissue engineering: physico-chemical properties and biological response of buffalo embryonic stem cells and transfectant of gfp-buffalo embryonic stem cells", *Acta Biomater*, VOL. 5, NO. 9, PP. 3453-3466, Nov. 2009.
- [9] M. Mami, A. Lucas-Girota, H. Oudadesse, R. Dorbez-Sridib, F. Mezahia, E. Dietrich , "Investigation of the surface reactivity of a sol-gel derived glass in the ternary system SiO₂-CaO-P₂O₅", *App Sur Sci*, VOL. 254, NO. 22, PP. 7386-7393, Sep. 2008.
- [10] S. Jebahi, H. Oudadesse, H. El Feki, T. Rebai, H. Keskes, P. Pellen, A. El Feki, "Antioxidative/oxidative effects of strontium-doped bioactive

- glass as bone graft. In vivo assays in ovariectomised rats," *J Appl Biomed*, VOL. 254, pp. 195–2097, Jan. 2012.
- [11] X. V. Bui, H. Oudadesse, Y. Le Gal, O. Merdrignac-Conanec, G. Cathelineau. "Bioactivity behaviour of biodegradable material comprising bioactive glass," *Korean J Chem Eng*, VOL. 29, NO. 2, PP. 215-220, Feb. 2012.
- [12] E. Dietrich, H. Oudadesse, M. Le Floch, B. Bureau, T. Gloriant. "In vitro Chemical Reactivity of Doped Bioactive Glasses: an Original Approach by Solid-State NMR Spectroscopy," *Adv Eng Mater*, VOL. 11, NO. 8, PP. B98–B105, Aug. 2009.
- [13] S. Jebahi, H. Oudadesse, X.V. Bui, H. Keskes, T. Rebai, A. El Feki, H. El Feki "Repair of bone defect using bioglass-chitosan as a pharmaceutical drug: An experimental study in an ovariectomised rat model". *Afr J Phar Pharm*, vol. 6, no. 16, pp. 1276 - 1287, Apr. 2012.
- [14] S. Jebahi, R. Nsiri, M. Boujbiha, E. Bouraga, T. Rebai, H. Keskes, A. El Feki, H. Oudadesse, H. El Feki "The impact of orthopedic device associated with carbonated hydroxyapatite on the oxidative balance: experimental study of bone healing rabbit model". *Eur J Orthop Surg Traumatol*. Oct. 2012. [Epub ahead of print].
- [15] K. H. Karlsson, R. Backman, M. Hupa "An equilibrium study of phosphate precipitation in bioactive glass," *Key Eng Mater*, vol. 220, pp. 103–7. 2002.
- [16] V. Banchet, J. Michel, E. Jallot, L. Wortham, S. Bouthors, D. Laurent-Maquin "Interfacial reactions of glasses for biomedical application by scanning transmission electron microscopy and microanalysis", *Acta Biomater*, vol. 2, No 3. pp. 349–59. May. 2006.
- [17] X. Lu, Y. Leng. "Theoretical analysis of calcium phosphate precipitation in simulated body fluid", *Biomaterials*, vol. 26, No10. pp. 1097–108. Apr. 2005.
- [18] S. Jebahi, M. Saoudi, R. Badraoui, H. Oudadesse, Z. Ellouz, H. Keskes, A. El Feki, H. El Feki, "Biologic Response to Carbonated Hydroxyapatite Associated with Orthopedic Device: Experimental Study in a Rabbit Model," *Kor J Path*, vol. 46, No1. pp. 48-54. JAN. 2012.
- [19] H. Oudadesse, E. Dietrich, Y. L. GAL, P. Pellen, B. Bureau, A.A. Mostapha, G. Cathelineau "Apatite forming ability and cytocompatibility of pure and Zn-doped bioactive glasses," *Biomed Mater*, vol. 6, no. 3, pp. 20, Jun. 2011.
- [20] E. Dietrich, H. Oudadesse, A. Lucas-Girot, M. Mami "In vitro bioactivity of melt-derived glass 46S6 doped with magnesium". *J Biomed Mater Res A*, vol. 88, no. 4, pp. 1087-96, Mar. 2009.
- [21] Neyman K. M., Rösch N. "Bonding and vibrations of CO molecules adsorbed at transition metal impurity sites on the MgO (001) surface. A density functional model cluster study", *Chemical Physics*, vol. 177, no. 2, pp. 561–570, Nov. 1993.
- [22] J.R. Jones, P. Sepulveda, L.L. Hench. "Dose dependent behavior of bioactive glass dissolution," *J Biomed Mater Res*, vol. 58, No 6, pp. 58:720, 2001.
- [23] M. Cerrutia, D. Greenspan, K. Powers. "Effect of pH and ionic strength on the reactivity of Bioglass 45S5". *Biomaterials*, vol. 26, no. 14, pp. 1665-74, May. 2005.
- [24] M. Ashok, N. Meenakshi Sundaram, S. Narayana Kalkura. "Crystallization of hydroxyapatite at physiological temperature". *Mater Lett*, vol. 57, no. 14, pp. 2066–2070, May. 2005.
- [25] Zhang Di, Mikko Hupa, Leena Hupa. "In situ pH within particle beds of bioactive glasses". *Acta Biomaterialia*, vol. 4, no. 5, pp. 1498-505, Sep. 2008.
- [26] L. L. Hench, R. J. Splinter, W. C. Allen, T. K. Greenlee. "Bonding mechanisms at the interface of ceramic prosthetic materials". *J Biomed Mater Res Symp*, vol. 5, no. 6, pp. 117–141, Nov. 1971.
- [27] M.G. Cerruti, D. Greenspan, K. Powers. "An analytical model for the dissolution of different particle size samples of bioglass in TRIS buffered solution", *Biomaterials*, vol. 26, no. 24, pp. 4903-11, Aug. 2005.
- [28] D.C. Greenspan, I.P. Zhong, G.P. La Torre. "Effect of surface area to volume ratio on in vitro surface reactions of bioactive glass particulates". *Bioceramics*, vol. 7, pp. 55–60, 1994.